



# Enhanced adsorption of salicylic acid onto a $\beta$ -naphthol-modified hyper-cross-linked poly(styrene-co-divinylbenzene) resin from aqueous solution

Jianhan Huang<sup>a,b,\*</sup>, Guan Wang<sup>a,b</sup>, Kelong Huang<sup>a,b</sup>

<sup>a</sup> School of Chemistry and Chemical Engineering, Central South University, Changsha 410083, China

<sup>b</sup> Key Laboratory of Resources Chemistry of Nonferrous Metals Ministry of Education, China

## ARTICLE INFO

### Article history:

Received 29 October 2010

Received in revised form 17 January 2011

Accepted 17 January 2011

### Keywords:

Hyper-cross-linked

Poly(styrene-co-divinylbenzene) resin

Adsorption

Isotherms

Kinetics

## ABSTRACT

A series of novel  $\beta$ -naphthol-modified hyper-cross-linked poly(styrene-co-divinylbenzene) resins were synthesized and the adsorption behaviors of the synthesized resins towards salicylic acid from aqueous solution was investigated. Among the synthesized five resins, HJ-G02 possessed the largest adsorption capacity towards salicylic acid. The molecular form of salicylic acid was favorable for the adsorption and mono-anion of salicylic acid can also be adsorbed by the resin. Low concentration of phenol posed a positive effect while high concentration of phenol posed a negative effect on the adsorption. The isotherms could be fitted by Freundlich model and the kinetic data could be characterized by pseudo-second-order rate equation. The breakthrough point of HJ-G02 towards salicylic acid was 108.8 BV and HJ-G02 could be regenerated by 1% of sodium hydroxide solution.

© 2011 Elsevier B.V. All rights reserved.

## 1. Introduction

Salicylic acid can be employed as a pharmaceutical intermediate to produce various medicines such as Aspirin, Fenamifuril, Salicylamide, Lopirin, Diflunisal and Benorylatum [1,2]. Salicylic acid at a low concentration can be acted as a kind of cosmetic while it will bring serious environmental problems at a high concentration. Salicylic acid can induce headache, nausea and it can even affect the liver and kidney. Moreover, biological degradation of salicylic acid is not feasible due to the electron-withdrawing carboxyl group on the benzene ring [3,4]. For these reasons, the efficient removal and recycling of salicylic acid from aqueous solution has received considerable attentions.

Macroporous cross-linked poly(styrene-co-divinylbenzene) (PS) and polymethacrylate resins have shown excellent adsorption properties towards aromatic compounds from aqueous solution, and hence they are frequently employed as efficient adsorbents to remove aromatic compounds from aqueous solution [5]. In particular, Davankov and Tsyurupa developed a hyper-cross-linking technique in the 1970s and synthesized a type of hyper-cross-linked PS resin from linear PS or low cross-linked PS using bi-functional cross-linking agents and Friedel-Crafts catalysts [6,7]. The specific surface area of the synthesized resin was shown to be relatively high with the pore diameter distribution being dominated by mesopores. Adsorption experiments

indicated that the synthesized resin displayed excellent adsorption properties towards non-polar and weakly polar aromatic compounds [8,9], whereas its adsorption capacity towards polar aromatic compounds such as salicylic acid and 4-aminobenzoic acid was relatively small [10,11]. Hence, in order to increase the adsorption capacities of the resin towards polar aromatic compounds, chemical modification is frequently considered by introducing some specific functional groups such as amino, amide, hydroxyl, carbonyl and carboxyl groups into the surface of the resin [12–15]. The results indicated that such chemically modified resins possessed an increased adsorption capacity towards polar aromatic compounds [13–15].

As macroporous cross-linked chloromethylated PS is applied as the reactant for the Friedel-Crafts reaction, meanwhile some aromatic compounds such as phenol [16] and  $\beta$ -naphthol are also added in the reaction mixture. In addition to the Friedel-Crafts reaction of the chloromethylated PS itself, the Friedel-Crafts reaction between the chloromethylated PS and  $\beta$ -naphthol will also occur simultaneously. Moreover, if different quantity of  $\beta$ -naphthol is added in the reaction mixture, the chemical structure as well as pore structure of the prepared resin will be distinctly different, and which results in a different adsorption selectivity of the prepared resin. To the best of our knowledge, there is no report focused on synthesis and adsorption behaviors of  $\beta$ -naphthol-modified hyper-cross-linked PS resin so far.

The object this study is composed of two aspects. The first one is synthesis of a series of  $\beta$ -naphthol-modified hyper-cross-linked PS resins from macroporous cross-linked chloromethylated PS by adding different quantity of  $\beta$ -naphthol in the Friedel-Crafts

\* Corresponding author. Tel.: +86 731 88879850; fax: +86 731 88879616.  
E-mail address: [xiaomeijiangou@yahoo.com.cn](mailto:xiaomeijiangou@yahoo.com.cn) (J. Huang).

reaction. The second one is the study of the adsorption behaviors of the  $\beta$ -naphthol-modified hyper-cross-linked PS resins towards salicylic acid from aqueous solution. HJ-G02 is selected as the polymeric adsorbent and the adsorption behaviors of HJ-G02 towards salicylic acid from aqueous solution are investigated.

## 2. Experimental method

### 2.1. Materials

Salicylic acid (molecular formula:  $C_6H_4(OH)(COOH)$ , molecular weight: 138.1), phenol and 4-aminobenzoic acid applied as the adsorbates were analytical reagents and used without further purification. Macroporous cross-linked chloromethylated PS was purchased from Langfang Chemical Co. Ltd. (Hebei, China). The Amberlite XAD-4 was kindly provided by Rohm & Haas Company (Philadelphia, USA) and X-5 was bought from the Chemical Plant of Nankai University (Tianjin, China).

### 2.2. Synthesis of $\beta$ -naphthol-modified hyper-cross-linked resins

As depicted in Scheme s1, 40 g of chloromethylated PS was swollen by 120 mL of nitrobenzene at room temperature over a period of 8 h and a small quantity of  $\beta$ -naphthol (0%, 2%, 5%, 10% or 15% relative to chloromethylated PS, w/w) dissolved by nitrobenzene was also added into the reaction mixture. Subsequently, 2.5 g of anhydrous zinc chloride was added into the reaction mixture at 323 K and the reaction mixture was heated to 388 K within 1 h. After retaining the reaction mixture at 388 K for ca. 8 h, the resulting solid particles were filtrated from the solution, rinsed with 1% of hydrochloric acid and anhydrous ethanol until the effluents from hydrochloric acid were transparent. Finally, the solid particles were washed with de-ionized water and extracted with ethanol for ca. 8 h to produce the  $\beta$ -naphthol-modified hyper-cross-linked resins, namely HJ-G00, HJ-G02, HJ-G05, HJ-G10 and HJ-G15.

### 2.3. Adsorption isotherms

In a cone-shaped flask with a stopper, about 0.1000 g of dry resin was accurately weighed and mixed with 50 mL of salicylic acid solution. The initial concentration of salicylic acid was set to be about 100–500 mg/L with 100 mg/L interval. 0.1 mol/L of hydrochloric acid or 0.1 mol/L of sodium hydroxide were applied to adjust the solution pH, 685.04 mg/L of phenol solution was used to investigate its effect on the adsorption. The flasks were then shaken in a thermostatic oscillator (its agitation speed was 150 rpm) for about 24 h at a desired temperature (288, 298, 308 or 318 K) until the adsorption equilibrium was reached, the concentration of the residual salicylic acid solution was measured and the equilibrium adsorption capacity of the resin towards salicylic acid was calculated as [17,18]:

$$q_e = \frac{(C_0 - C_e)V}{W} \quad (1)$$

where  $q_e$  is equilibrium adsorption capacity (mg/g),  $C_0$  and  $C_e$  are the initial and equilibrium concentration of salicylic acid (mg/L),  $V$  is the volume of the solution (L) and  $W$  is the weight of the resin (g).

### 2.4. Kinetic curves

About 1.0000 g of the resin and 500 mL of salicylic acid solution with concentration of 396.5 mg/L were quickly introduced into a cone-shaped flask and continuously shaken at a desired temperature (288, 298, 308 or 318 K). 0.5 mL of the solution was sampled at different time intervals and the concentration of the residual salicylic acid was determined until the adsorption equilibrium was

reached, the adsorption capacity of the resin towards salicylic acid at contact time  $t$  was calculated as:

$$q_t = \frac{(C_0 - C_t)V}{W} \quad (2)$$

where  $q_t$  is the adsorption capacity at contact time  $t$  (mg/g) and  $C_t$  is the concentration of salicylic acid at contact time  $t$  (mg/L).

### 2.5. Dynamic adsorption and desorption

The fixed-bed column experiment for the adsorption of the resin towards salicylic acid was carried out by a glass column (16 mm of diameter and 290 mm of length) at 298 K. 10 mL of wet resin was packed in the glass column and a HL-2 pump (Shanghai Huxi Analysis Instrument Factory Co. Ltd., China) was used to ensure a constant flow rate. 500.0 mg/L of salicylic acid was passed through the column at a flow rate of 5.8 BV/h (1 BV = 10 mL) and the respective concentration of salicylic acid from the effluent was recorded until it was equal to the inlet concentration (the breakthrough point was recorded at 5% of the inlet concentration). Subsequently, the resin column was rinsed by de-ionized water until the concentration of salicylic acid from the effluent was zero, and 1% of sodium hydroxide solution was applied to regenerate the resin.

### 2.6. Analysis

The pore structure of the resin was determined by  $N_2$  adsorption-desorption isotherms measured at 77 K via a Micromeritics Tristar 3000 surface area and porosity analyzer (Micromeritics Corp., Norcross, GA, USA). These allowed the specific surface area, pore volume and pore diameter distribution of the resin to be calculated. Before performing such experiment, the resin was pre-treated by exposure to  $N_2$  gas 24 h so that any water and other impurities present in the material were displaced. The specific surface area and pore volume of the resin were calculated according to Brunauer–Emmett–Teller (BET) model and the pore diameter distribution of the resin was calculated by applying BJH (Barrett, Joyner and Halenda) method to the  $N_2$  desorption data. The Fourier transform infrared ray (FTIR) spectrum of the resin was collected on a Nicolet 510P Fourier transform infrared instrument (Thermo Nicolet Corporation, USA) via KBr disk method. The concentration of salicylic acid was measured via a UV-2450 spectrophotometer (Shimadzu Coop., Nakagyo-ku, Kyoto, Japan) at a wavelength of 296.5 nm [17].

## 3. Results and discussion

### 3.1. Characterization of the resin

Fig. s1(a) displays the specific surface area and pore volume of the prepared resins. The specific surface area of the five resins has the same trend as the pore volume. The specific surface area of HJ-G00 is the highest among the five resins and it decreases as adding  $\beta$ -naphthol in the Friedel–Crafts reaction.

Fig. s1(b) describes the  $N_2$  adsorption-desorption isotherms of HJ-G00, HJ-G02, HJ-G05, HJ-G10 and HJ-G15, respectively. All of the adsorption isotherms seem close to type-II [19]. At the initial part of the adsorption isotherm with a relative pressure below 0.05, the  $N_2$  adsorption capacity increases sharply with increasing the relative pressure, proving that micropores are existent (the micropore specific surface areas of these resins are determined to be 538.5, 429.1, 474.7, 296.1 and 326.3  $m^2/g$ , respectively). The visible hysteresis loops of the desorption isotherm indicate that mesopores are also existent. These analyses agree with the pore diameter distribution in Fig. s1(c). In addition, it can be observed that the Friedel–Crafts reaction results in a great transfer for the pore diameter distribu-

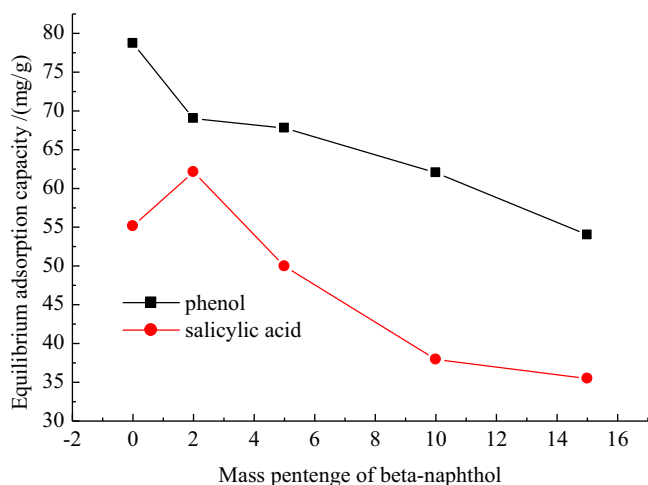


**Fig. 1.** Comparison of adsorption capacity of HJ-G00, HJ-G02, HJ-G05, HJ-G10 and HJ-G15 towards phenol and salicylic acid from aqueous solution.

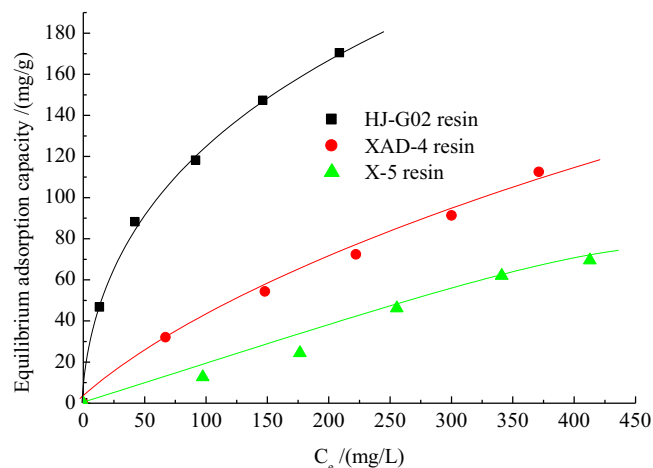
tion of the resin, mesopores and macropores are the main pores for the chloromethylated PS and the average pore diameter is 25.7 nm, while mesopores in the range of 2–5 nm play a predominant role for the  $\beta$ -naphthol-modified hyper-cross-linked resins and the average pore diameters of the five resins are given to be 2.41, 2.45, 2.42, 2.53 and 2.55 nm, respectively.

Fig. s1(d) is the FTIR spectra of the chloromethylated PS and the five hyper-cross-linked resins. Two strong vibrations of the  $\text{CH}_2\text{Cl}$  groups with frequencies at 1265 and 669  $\text{cm}^{-1}$  are greatly weakened after the Friedel-Crafts reaction [20], while the appearance of some other typical vibrations may be noticed for the five hyper-cross-linked resins. First of all, a vibration with a frequency at 1704  $\text{cm}^{-1}$  appears, and this vibration may be related to C=O stretching of the formaldehyde carbonyl groups. The appearance of this vibration may arise from the oxidation of benzyl chloride [21,22]. Secondly, a strong absorption band occurs at 3446  $\text{cm}^{-1}$  after loading  $\beta$ -naphthol on the hyper-cross-linked resin, and this absorption band may be concerned with O–H stretching of  $\beta$ -naphthol. Moreover, the absorption related to the O–H stretching is gradually strengthened with increment the  $\beta$ -naphthol quantity added in the Friedel-Crafts reaction. At last, the characteristic C=C stretching of the benzene ring at 1604, 1505 and 1446  $\text{cm}^{-1}$  is strengthened after the reaction [20]. These results demonstrate that  $\beta$ -naphthol has been loaded successfully on the surface of the hyper-cross-linked resins.

### 3.2. Adsorption selectivity

Fig. 1 compares the adsorption capacities of HJ-G00, HJ-G02, HJ-G05, HJ-G10 and HJ-G15 towards phenol and salicylic acid, respectively. It is obvious that HJ-G00 holds the largest adsorption capacity towards phenol among the five resins while HJ-G02 possesses the largest adsorption capacity towards salicylic acid, displaying the different adsorption selectivity. HJ-G02 is chosen in this study to investigate the adsorption behaviors towards salicylic acid from aqueous solution.

The specific surface areas of HJ-G00, HJ-G02, HJ-G05, HJ-G10 and HJ-G15 are measured to be 889.0, 766.8, 559.0, 566.1 and 588.1  $\text{m}^2/\text{g}$ , respectively, and the micropore specific surface areas of these resins are all a little higher than 50% of the total specific surface areas. In addition, the average pore diameters of the five resins are all 2–6 times larger than the molecular size of salicylic acid (the molecular size of salicylic acid is predicted to be 0.69 nm  $\times$  0.46 nm by GAUSSIAN 03 program). These relationships are favorable for the adsorbate–adsorbate interaction via pore fill-



**Fig. 2.** Comparison of adsorption isotherms of HJ-G02, XAD-4 and X-5 towards salicylic acid from aqueous solution at 288 K.

ing mechanism. In general, the specific surface area, polarity and pore structure of the adsorbent are thought to be the main factors influencing the adsorption [19,23]. The greatly high specific surface area especially the micropore specific surface area of HJ-G00 induces the largest adsorption capacity of HJ-G00 towards phenol from aqueous solution. The polar formaldehyde carbonyl and phenolic hydroxyl groups are loaded on HJ-G02, and salicylic acid is also a polar molecule with polar phenolic hydroxyl and carboxyl groups. There should be some specific polar interaction between HJ-G02 and salicylic acid, and which enhances the adsorption of HJ-G02 towards salicylic acid.

### 3.3. Comparison of adsorption of different adsorbates onto HJ-G02 from aqueous solution

The adsorption isotherms of HJ-G02 towards phenol, salicylic acid and 4-aminobenzoic acid are measured and the results are displayed in Fig. s2. It is observed that the adsorption of HJ-G02 towards phenol is comparable with salicylic acid, while the adsorption of HJ-G02 towards 4-aminobenzoic acid is much diminished in comparison with phenol and salicylic acid, and hence salicylic acid is applied as the adsorbate in this study.

### 3.4. Comparison of adsorption of salicylic acid onto different resins from aqueous solution

The commercial XAD-4 and X-5 are both polystyrene resins with high hydrophobicity [24], and they are both considered to be the most efficient polymeric adsorbents for removing aromatic pollutants from wastewater, especially for non-polar and weakly polar aromatic pollutants such as  $\beta$ -naphthol and phenol [25]. Thus, the adsorption isotherm of HJ-G02 towards salicylic acid is compared with XAD-4 and X-5 (Fig. 2). Fig. 2 indicates that the adsorption capacity of HJ-G02 towards salicylic acid is much larger than XAD-4 and X-5 at the same equilibrium concentration and temperature. The specific surface area of HJ-G02 (766.8  $\text{m}^2/\text{g}$ ) is a little lower than that of XAD-4 (873.1  $\text{m}^2/\text{g}$ ) and higher than that of X-5 (551.2  $\text{m}^2/\text{g}$ ). The larger adsorption capacity of HJ-G02 towards salicylic acid in comparison with XAD-4 may be from the loading of formaldehyde carbonyl and phenolic hydroxyl groups on HJ-G02, while the much enhanced adsorption of HJ-G02 compared with X-5 may be resulted from the combinations of the specific surface area and the polarity interaction.

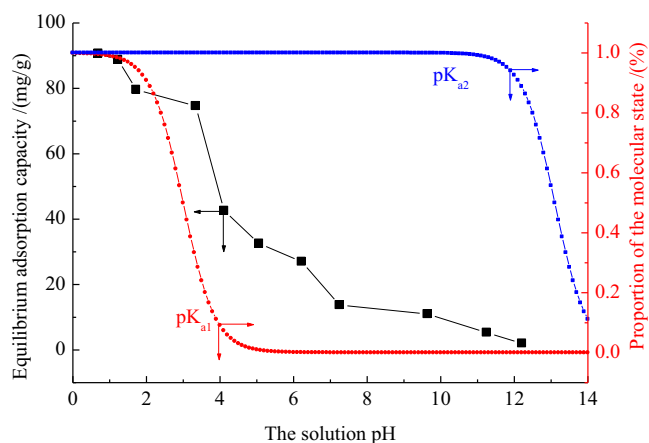


**Fig. 3.** Effect of the solution pH on the adsorption of HJ-G02 towards salicylic acid from aqueous solution.

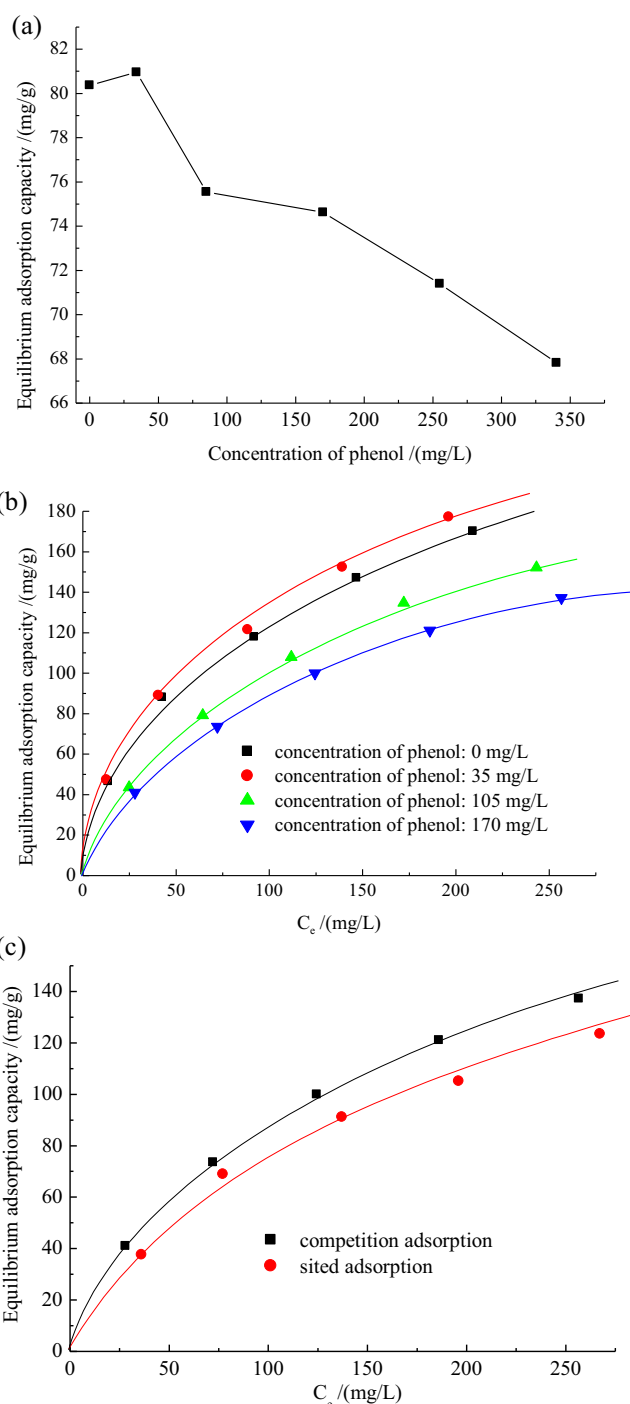
### 3.5. Effect of the solution pH on the adsorption

Fig. 3 shows the effect of the solution pH on the adsorption of HJ-G02 towards salicylic acid.  $pK_{a1}$  and  $pK_{a2}$  of salicylic acid are given to be 2.98 and 13.1, respectively [20], and hence the dissociation curves of salicylic acid are predicted and also shown in Fig. 3. It is seen that the adsorption of salicylic acid onto HJ-G02 has the same trend as the dissociation curve of salicylic acid, implying that the molecular form of salicylic acid is suitable for the adsorption [15,23]. As the solution pH is lower than 2.98, the ionization of salicylic acid will be affected and more salicylic acid molecules will be obtained, hence the adsorption of salicylic acid is strengthened. As the solution pH is higher than 2.98, salicylic acid will be gradually ionized to mono-anion and even di-anion, the proportion of salicylic acid molecules will decrease, inducing the adsorption weakened. In particular, it is seen that the adsorption capacity of HJ-G02 is not zero even if the proportion of the molecular state of salicylic acid is zero when pH is more than 6 (see the dissociation curve of salicylic acid as  $pK_{a1}$  is applied in the prediction). That is, HJ-G02 can adsorb the mono-anion of salicylic acid, but cannot adsorb di-anion of salicylic acid.

### 3.6. Effect of phenol on the adsorption

Phenol is inevitably existent in salicylic acid wastewater, and hence the effect of phenol on the adsorption should be considered. As shown in Fig. 4(a), low concentration of phenol (<35 mg/L) poses a positive effect while high concentration of phenol poses a negative effect on the adsorption. The solubility of phenol in water is much higher than salicylic acid (9.3 and 0.22 g/100 mL  $H_2O$  for phenol and salicylic acid, respectively [20]). As adding a small quantity of phenol in salicylic acid solution, a large number of water molecules will be “trapped” from the surrounding of salicylic acid to surround phenol due to the much higher solubility of phenol in water. These “trapped” water molecules are used to dissolve phenol. This process will result in greater “pseudo” hydrophobicity of salicylic acid, and which induces a larger adsorption capacity towards salicylic acid on the resin [26]. As the concentration of phenol in the solution is enough high, the competition adsorption of phenol on the resin can not be ignored, and the adsorption of salicylic acid on the resin should be reduced.

To further investigate the effect of phenol on the adsorption, different concentrations of phenol (0, 35, 105 and 170 mg/L) are combined with the series of standard solution of salicylic acid, and the adsorption isotherms of salicylic acid are measured (competition adsorption in Fig. 4(b)). Fig. 4(b) agrees with Fig. 4(a) that



**Fig. 4.** Effect of concentration of phenol on the adsorption at 298 K (a) the concentration of phenol applied was 685.04 mg/L; (b) in the competition adsorption, the initial concentration of phenol was 0, 35, 105 and 170 mg/L; (c) in the sited adsorption, firstly 50 mL of phenol solution with a concentration of 170 mg/L was applied for HJ-G02. After the adsorption of HJ-G02 towards phenol was completed, the residual phenol solution was removed, and the HJ-G02 was subjected to salicylic acid solution.

low concentration of phenol leads an increased adsorption capacity towards salicylic acid whereas high concentration of phenol results in a decreased one. Langmuir and Freundlich models are two typical models to describe the adsorption process. Langmuir model can be given as [27]:

$$\frac{C_e}{q_e} = \frac{C_e}{q_m} + \frac{1}{q_m K_L} \quad (3)$$



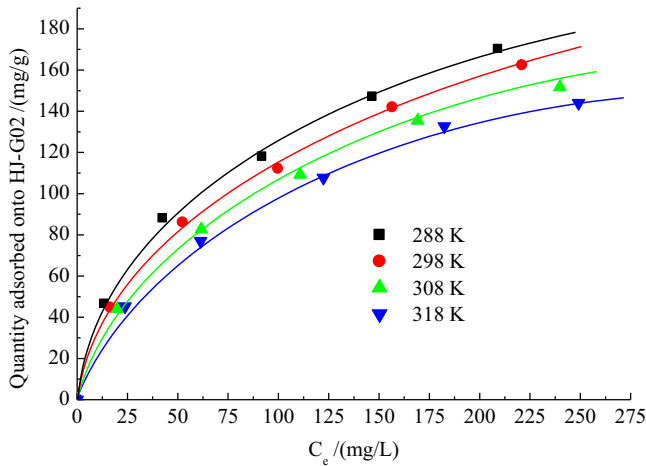


Fig. 5. Adsorption isotherms of HJ-G02 towards salicylic acid from aqueous solution.

where  $q_m$  is the maximum adsorption capacity (mg/g) and  $K_L$  is a characteristic constant (L/mg).

The Freundlich model can be rearranged as [28]:

$$\log q_e = \frac{1}{n} \log C_e + \log K_F \quad (4)$$

where  $K_F$  [(mg/g)(L/mg)<sup>1/n</sup>] and  $n$  (dimensionless) are the characteristic constants.

The corresponding parameters  $K_L$ ,  $K_F$  and  $n$ , as well as the correlation coefficients  $R^2$  are summarized in Table s1 (Fig. s4). The adsorption data can be fitted by both of Langmuir and Freundlich models since  $R^2 > 0.98$ . With increasing the concentration of phenol, the  $K_L$  and  $K_F$  values firstly increase and then decrease, accordant with the adsorption capacity.

If the adsorption of HJ-G02 towards phenol is firstly performed, can HJ-G02 which has adsorbed phenol still adsorb salicylic acid from aqueous solution? Therefore, we have carried out this experiment (sited adsorption, Fig. 4(c)). Comparing the results of the competition adsorption with those of the sited adsorption, it is seen that the values of  $q_m$ ,  $K_L$  and  $K_F$  in the sited adsorption decrease rapidly in comparison with those in the competition adsorption (Fig. s5), implying that the interaction between the resin and the adsorbate is weakened and some adsorption sites on the resin have been occupied by phenol as phenol is existent in the solution.

### 3.7. Adsorption isotherms

As shown in Fig. 5, the adsorption capacity of HJ-G02 towards salicylic acid decreases with increasing the temperature, suggesting an exothermic process [19]. Langmuir and Freundlich models are adopted to describe the adsorption data, the corresponding parameters  $K_L$ ,  $K_F$  and  $n$ , as well as the correlation coefficients  $R^2$  are listed in Table s2 (Fig. s6). It is seen that the isotherm data can be fitted by Langmuir and Freundlich models since  $R^2 > 0.98$  and Freundlich model is more suitable for the adsorption.

According to the Clausius-Clapeyron equation [13]:

$$\frac{d \ln C_e}{dT} = \frac{\Delta H}{RT^2} \quad (5)$$

where  $\Delta H$  is the adsorption enthalpy (kJ/mol) and  $R$  is the ideal gas constant. Eq. (5) can be followed by an integral method below:

$$\ln C_e = -\frac{\Delta H}{RT} + C' \quad (6)$$

where  $C'$  is the integral constant. By plotting  $\ln C_e$  against  $1/T$  (Fig. s7), it is found that the isosters of  $\ln C_e$  against  $1/T$  can be fitted

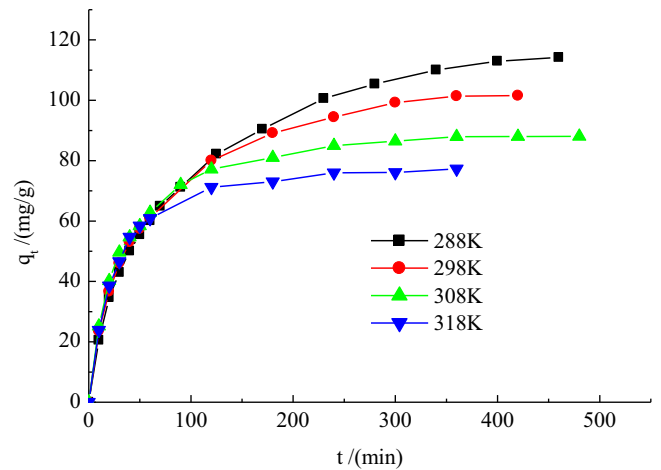


Fig. 6. Adsorption kinetic curves of HJ-G02 towards salicylic acid from aqueous solution.

to straight lines, and  $\Delta H$  can be calculated from the slopes of the straight lines.

Adsorption free energy at a low solute concentration can be calculated as [29]:

$$\Delta G = -RT \int_0^x q \frac{dx}{x} \quad (7)$$

where  $\Delta G$  is the adsorption free energy (kJ/mol),  $q$  is the adsorption capacity onto the adsorbent (mg/g), and  $x$  is the mole fraction of the adsorbed solute in the solution. As the adsorption can be characterized by Freundlich isotherm model, incorporating Eq. (4) into Eq. (7) will yield:

$$\Delta G = -nRT \quad (8)$$

where  $n$  is the characteristic constant in Freundlich isotherm model.

Adsorption entropy  $\Delta S$  (J/(molK)) can be calculated by Gibbs-Helmholtz equation:

$$\Delta S = \frac{\Delta H - \Delta G}{T} \quad (9)$$

Table s3 lists the  $\Delta H$ ,  $\Delta G$  and  $\Delta S$  of HJ-G02 towards salicylic acid from aqueous solution. The value of  $\Delta H$  is negative, indicating an exothermic process [19]. The value of  $\Delta H$  decreases with increasing the adsorption capacity resulted from the surface energetic heterogeneity of HJ-G02 [13,18]. The value of  $\Delta G$  is also negative, indicating that the adsorption is a spontaneous process. The value of  $\Delta S$  is negative, revealing that a more ordered arrangement of salicylic acid is shaped on the surface of HJ-G02 after the adsorption.

### 3.8. Adsorption kinetic curves

As can be seen from Fig. 6, the adsorption can reach equilibrium within 400 min and a higher temperature needs a shorter required time from the beginning to the equilibrium while with a smaller adsorption capacity. In general, the pseudo-second-order rate equation is appropriate for the whole adsorption process, hence in the present study it is employed to fit the adsorption kinetic data, its linear form is [30]:

$$\frac{t}{q_t} = \frac{1}{k_2 q_e^2} + \frac{t}{q_e} \quad (10)$$

where  $k_2$  is the pseudo-second-order rate constant (g/(mg min)).

Plotting of  $t/q_t$  versus  $t$  for the adsorption is depicted in Fig. s8 and the fitted correlation parameters are summarized in Table s4.

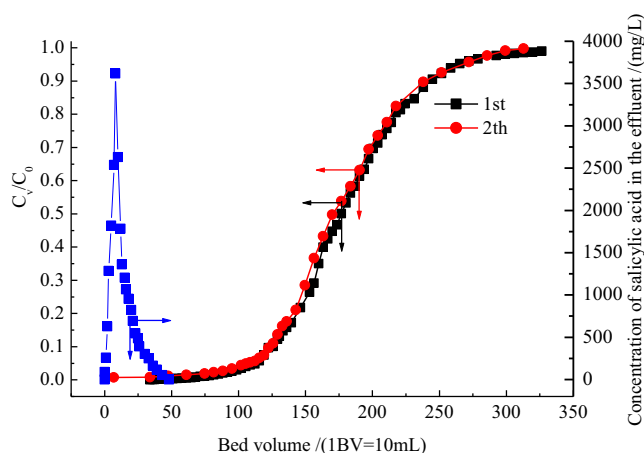


Fig. 7. The dynamic adsorption and desorption curves of HJ-G02 towards salicylic acid from aqueous solution.

It is clear that the pseudo-second-order rate equation characterizes the adsorption well with  $R^2 > 0.99$ . In particular, the adsorption at a higher temperature has a greater pseudo-second-order rate constant, accordant with the above observation that the required time at a higher temperature is shorter.

In addition, the initial adsorption rate ( $h$ , mg/(g min)) and half-adsorption time ( $t_{1/2}$ , min) can be calculated as:

$$h = k_2 q_e^2 \quad (11)$$

$$t_{1/2} = \frac{1}{k_2 q_e} \quad (12)$$

It is observed that the initial adsorption rate at a higher temperature is greater and the required half-adsorption time at a higher temperature is much shorter.

The apparent activation energy  $E_a$  (kJ/mol) can be calculated via the Arrhenius equation as:

$$\ln k_2 = -\frac{E_a}{RT} + \ln k_0 \quad (13)$$

where  $k_0$  is a constant. Plot of  $\ln k_2$  versus  $1/T$  (Fig. s9), a straight line is obtained, and  $E_a$  can be calculated from the slope of straight line to be 41.35 kJ/mol.

In common, the intra-particle diffusion is the rate-limiting step for the adsorption of hyper-cross-linked resin towards aromatic compounds from aqueous solution [29]. Therefore, the kinetic data are further dealt with by the intra-particle diffusion model proposed by Weber and Morris [31]:

$$q_t = k_d t^{1/2} + C \quad (14)$$

where  $k_d$  is the intra-particle diffusion rate (mg/(g min<sup>1/2</sup>)), and  $C$  is a constant.

If plotting of  $q_t$  versus  $t^{1/2}$  gives a straight line and the straight line passes through the origin, the intra-particle diffusion is the rate-limiting step for the adsorption. While if it presents a multi-linear relationship or does not pass through the origin, two or more diffusion mechanisms affect the adsorption [32]. Fig. s10 is the plotting of  $q_t$  versus  $t^{1/2}$  for the adsorption, and it is found that they yield a three-stage process. At the initial stage, it poses a linear relationship and the straight lines pass through the origin, indicating that the intra-particle diffusion is the rate-limiting step. Moreover, the  $k_{d1}$  presents an order as  $k_{d1(288\text{ K})} < k_{d1(298\text{ K})} < k_{d1(308\text{ K})} < k_{d1(318\text{ K})}$ , implying that the adsorption rate at a higher temperature is greater. At the second stage, plots of  $q_t$  versus  $t^{1/2}$  also yield linear relationships but do not pass through the origin, revealing that multi-diffusion mechanisms are involved.

### 3.9. Dynamic adsorption and desorption

The result of the fixed-bed column dynamic adsorption of HJ-G02 towards salicylic acid from aqueous solution is shown in Fig. 7, where  $C_v$  is the concentration at different bed volume of the effluent (mg/L). It is seen that the breakthrough point of salicylic acid is 108.8 BV, which indicates that HJ-G02 is an efficient polymeric adsorbent for adsorptive removal of salicylic acid from aqueous solution. When 1% of sodium hydroxide aqueous solution is used to desorb the adsorbed salicylic acid on HJ-G02 resin column, HJ-G02 can be regenerated by sodium hydroxide. A continuous adsorption-regeneration run of the used HJ-G02 resin column is performed and the second cycle is almost identical with the first cycle, implying that HJ-G02 can be regenerated and its repeated use is feasible.

## 4. Conclusions

A series of  $\beta$ -naphthol-modified hyper-cross-linked PS resins had been synthesized and HJ-G02 possessed the largest adsorption capacity towards salicylic acid from aqueous solution. HJ-G02 had considerable adsorption selectivity and it was superior to the commercial XAD-4 and X-5. The molecular form of salicylic acid was favorable for the adsorption and mono-anion of salicylic acid could also be adsorbed on the resin. Low concentration of phenol was favorable while a high concentration of phenol was negative for the adsorption. Freundlich model depicted the isotherms better than Langmuir one and the values of the adsorption enthalpy, free energy and entropy were all negative. The pseudo-second-order rate equation characterized the kinetic curves well and the intra-particle diffusion was the rate-limiting step at the initial process. The breakthrough point of HJ-G02 towards salicylic acid was 108.8 BV and HJ-G02 could be regenerated by 1% of sodium hydroxide solution.

## Acknowledgments

The research was supported by the National Natural Science Foundation of China (No. 20804058), the Third Shenghua Yuying Project of Central South University and Open-End Fund for the Valuable and Precision Instruments of Central South University.

## Appendix A. Supplementary data

Supplementary data associated with this article can be found, in the online version, at doi:10.1016/j.cej.2011.01.065.

## References

- [1] R.S. Juang, J.Y. Shiau, H.J. Shao, Effect of temperature on equilibrium adsorption of phenols onto nonionic polymeric resins, Sep. Sci. Technol. 34 (1999) 1819–1831.
- [2] M. Otero, C.A. Grande, A.E. Rodrigues, React. Funct. Polym. 60 (2004) 203–208.
- [3] D.M. Meier, A. Urakawa, A. Baiker, Adsorption behavior of salicylic, benzoic, and 2-methyl-2-hexenoic acid on alumina: an in situ modulation excitation PM-IRRAS study, Phys. Chem. Chem. Phys. 11 (2009) 10132–10139.
- [4] L. Khenniche, F. Aissani, Preparation and characterization of carbons from coffee residue: adsorption of salicylic acid on the prepared carbons, J. Chem. Eng. Data 55 (2010) 728–734.
- [5] B. Saha, M. Streat, Adsorption of trace heavy metals: application of surface complexation theory to a macroporous polymer and a weakly acidic ion-exchange resin, Ind. Eng. Chem. Res. 44 (2005) 8671–8681.
- [6] G.I. Rozenberg, A.S. Shabaeva, V.S. Moryakov, T.G. Musin, M.P. Tsyurupa, V.A. Davankov, Sorption properties of hypercrosslinked polystyrene sorbents, React. Polym. Ion Exchang. Sorb. 1 (1983) 175–182.
- [7] L.D. Belyakova, T.I. Shevchenko, V.A. Davankov, M.P. Tsyurupa, Sorption of vapors of various substances by hypercrosslinked “styrosorb” polystyrenes, Adv. Colloid Interface Sci. 25 (1986) 249–266.
- [8] B. Saha, E. Karounou, M. Streat, Removal of 17- $\alpha$ -oestradiol and 17- $\beta$ -oestradiol from water by activated carbons and hypercrosslinked polymeric phases, React. Funct. Polym. 70 (2010) 531–544.

- [9] N.E. Oro, C.A. Lucy, Comparison of hypercrosslinked polystyrene columns for the separation of nitrogen group-types in petroleum using high performance liquid chromatography, *J. Chromatogr. A* 1217 (2010) 6178–6185.
- [10] C. Valderrama, J.I. Barios, M. Caetano, A. Farran, J.L. Cortina, Kinetic evaluation of phenol/aniline mixtures adsorption from aqueous solutions onto activated carbon and hypercrosslinked polymeric resin (MN200), *React. Funct. Polym.* 70 (2010) 142–150.
- [11] M.P. Tsyurupa, L.A. Maslova, A.I. Andreeva, T.A. Mrachkovskaya, V.A. Davankov, Sorption of organic compounds from aqueous media by hypercrosslinked polystyrene sorbents "Styrosorb", *React. Polym.* 25 (1995) 69–78.
- [12] Y. Li, C. Long, W.H. Tao, A.M. Li, Q.X. Zhang, Fractal dimensions of macroporous and hypercrosslinked polymeric adsorbents from nitrogen adsorption data, *J. Chem. Eng. Data* 55 (2010) 3147–3150.
- [13] H.T. Li, Y.C. Jiao, M.C. Xu, Z.Q. Shi, B.L. He, Thermodynamics aspect of tannin sorption on polymeric adsorbents, *Polymer* 45 (2004) 181–188.
- [14] B.C. Pan, W.M. Zhang, B.J. Pan, H. Qiu, Q.R. Zhang, Q.X. Zhang, S.R. Zheng, Efficient removal of aromatic sulfonates from wastewater by a recyclable polymer: 2-naphthalene sulfonate as a representative pollutant, *Environ. Sci. Technol.* 42 (2008) 7411–7416.
- [15] W.M. Zhang, C.H. Hong, B.C. Pan, Q.J. Zhang, P.J. Jiang, K. Jia, Removal enhancement of 1-naphthol and 1-naphthylamine in single and binary aqueous phase by acid-basic interactions with polymer adsorbents, *J. Hazard. Mater.* 158 (2008) 293–299.
- [16] B.L. He, H.S. Wang, Q.X. Zhang, Z.Q. Shi, X.Q. Guo, X.B. Li, Synthesis and adsorption properties of a novel polymeric adsorbent for removal of phenols, *Acta Polym. Sin.* 5 (1983) 356–361.
- [17] L. Khenniche, F. Aissani, Characterization and utilization of activated carbons prepared from coffee residue for adsorptive removal of salicylic acid and phenol: kinetic and isotherm study, *Desal. Water Treat.* 11 (2009) 192–203.
- [18] J.H. Huang, C. Yan, K.L. Huang, Removal of *p*-nitrophenol by a water-compatible hypercrosslinked resin functionalized with formaldehyde carbonyl groups and XAD-4 from aqueous solution: a comparative study, *J. Colloid Interface Sci.* 332 (2009) 60–64.
- [19] B.L. He, W.Q. Huang, *Ion Exchange and Adsorption Resin*, Shanghai Science and Technology Education Press, Shanghai, 1995.
- [20] J.T. Wang, Q.M. Hu, B.S. Zhang, Y.M. Wang, *Organic Chemistry*. Nankai University Press, Tianjing, 1998.
- [21] G.H. Meng, A.M. Li, W.B. Yang, F.Q. Liu, X. Yang, Q.X. Zhang, Mechanism of oxidative reaction in the postcrosslinking of hypercrosslinked polymers, *Eur. Polym. J.* 43 (2007) 2732–2737.
- [22] M.C. Xu, Z.Q. Shi, B.L. He, Structure and adsorption properties of hypercrosslinked polystyrene adsorbents, *Acta Polym. Sin.* 4 (1996) 446–449.
- [23] J.H. Huang, K.L. Huang, S.Q. Liu, A.T. Wang, C. Yan, Adsorption of Rhodamine B and methyl orange on a hypercrosslinked polymeric adsorbent in aqueous solution, *Colloids Surf. A* 330 (2008) 55–61.
- [24] Y. Ku, K.C. Lee, Removal of phenols from aqueous solution by XAD-4 resin, *J. Hazard. Mater.* 80 (2000) 59–68.
- [25] K.L. Hubbard, J.A. Finch, G.D. Darling, The preparation and characteristics of poly(styrene-co-ethylvinylbenzene), including Ambeflite XAD-4, styrenic resins with pendent vinylbenzene groups, *React. Funct. Polym.* 36 (1998) 17–30.
- [26] A.C. Breyer, W.III. Rieman, Salting-out chromatography. VI. Effect of the length of the hydrocarbon chain, the eluent salt, and the cross-linking and ionic form of the resin, *Talanta* 4 (1960) 67–74.
- [27] A.P. Gaunce, P.A. Anastassiadis, An estimation of the noneluted dye-protein complex from paper electropherograms through the application of Langmuir's isotherm equation, *Anal. Biochem.* 17 (1966) 357–364.
- [28] E.A. Walker, P. Morton, The application of the Freundlich isotherm to the adsorption of sugars from solution by a column of charcoal, *Analyst* 89 (1964) 512–519.
- [29] K. Zheng, B.C. Pan, Q.J. Zhang, W.M. Zhang, B.J. Pan, Y.H. Han, Q.R. Zhang, W. Du, Z.W. Xu, Q.X. Zhang, Enhanced adsorption of *p*-nitroaniline from water by a carboxylated polymeric adsorbent, *Sep. Purif. Technol.* 57 (2007) 250–256.
- [30] S. Lagergren, Zur, Theorie der sogenannten adsorption geloster stoffe, *K. Sven. Vetenskapsakad. Handl.* 24 (1898) 1–18.
- [31] W.J. Weber, J.C. Morris, *J. Sanit. Eng. Div. Am. Soc. Civ. Eng.* 89 (1963) 31–60.
- [32] Z.L. Zhu, A.M. Li, L. Yan, F.Q. Liu, Q.X. Zhang, Preparation and characterization of highly mesoporous spherical activated carbons from divinylbenzene-derived polymer by ZnCl<sub>2</sub> activation, *J. Colloid Interface Sci.* 316 (2007) 628–634.